Modelling of thermal transport in wire + arc additive manufacturing process

E. A. Bonifaz
Mechanical Engineering Department, Universidad San Francisco de Quito, Cumbayá-Ecuador
ebonifaz@usfq.edu.ec

Abstract

Due to the simultaneous effects of different physical phenomena that occur on different length and time scales, modelling the fusion and heat affected microstructure of an Additive Manufacturing (AM) process requires more than intelligent meshing schemes to make simulations feasible. The purpose of this research was to develop an efficient high quality and high precision thermal model in wire + arc additive manufacturing process. To quantify the influence of the process parameters and materials on the entire welding process, a 3D transient non-linear finite element model to simulate multi-layer deposition of cast IN-738LC alloy onto SAE-AISI 1524 Carbon Steel Substrates was developed. Temperature-dependent physical properties and the effect of natural and forced convection were included in the model. A moving heat source was applied over the top surface of the specimen during a period of time that depends on the welding speed. The effect of multi-layer deposition on the prediction and validation of melting pool shape and thermal cycles was also investigated. The heat loss produced by convection and radiation in the AM layers surfaces were included into the finite element analysis. As the AM layers itself act as extended surfaces (fins), it was found that the heat extraction is quite significant. The developed thermal model is quite accurate to predict thermal cycles and weld zones profiles. A firm foundation for modelling thermal transport in wire + arc additive manufacturing process it was established.

Keywords: Multi-layer deposition, weld pool, thermal cycles, layer build-up process, heat source.

1 Introduction

Additive Manufacturing (AM) involves a comprehensive integration of materials science, mechanical engineering and joining technologies. Related literature [1-6] contains plenty information on energy insertion, dynamics of the molten pool, and mechanical properties generated by the evolution of thermal (residual) stresses. Directed Energy Deposition (DED) process predominantly used with metals in the form of either powder or wire, is often referred to as "metal deposition" technology [7]. DED encompasses all processes that use a laser, arc or e-beam heat source to generate a melt pool into which feedstock (powder or wire) is deposited. Wire + arc additive manufacturing (WAAM) process is essentially an extension of welding process. The origins of this category can be traced to welding technology, where material can be deposited outside a build environment by flowing a shield gas over the melt pool [8]. WAAM is a layer-by-layer build-up procedure that can be categorized as a form of multipass arc-welding for additive manufacturing (AM) purposes. In multipass welding, multiple welds interact in a complex thermomechanical manner. In the AM welding procedure, the current metal layers are deposited on top of previously solidified weld beads. Complex geometries and assemblies, weight reduction, rapid design iterations, creation of new graded materials with improved material properties, minimization of lead time and material waste, elimination of tooling, and component repair, are some of the numerous advantages to AM over traditional subtractive manufacturing. A component manufactured by the AM "welding" procedure can achieve equivalent mechanical properties to a forged or cast complex component. However, the surface finish, the accuracy to ensure a constant quality during the build-process, resulting in e.g. varying porosity throughout the part, and the high residual stresses that arise during manufacturing, are questionable. For instance, residual stresses may limit the load resistance and contribute to the formation of thermal cracks [4]. Therefore, to produce a high-quality part or product, it is important to establish a methodology for characterizing direct energy deposited metals by linking processing variables to the resulting microstructure and subsequent material properties.

Temperature history and thermal cycles during DED directly dictate the weld pool dimensions and resulting microstructure. However, the temperature magnitude and the molten pool size are very challenging to measure and control due to the transient nature and small size of the molten pool. Of this manner, modelling is needed to enable development of predictive relationships between material microstructure, material properties, and the resulting material lifecycle performance. The prediction of material lifecycle performance as a function of composition and processing parameters for DED-AM methods represents a grand challenge and consequently research in the following topics are necessary: 1) Prediction of microstructure evolution during single and multiple laser, arc, or e-beam passes 2) Prediction of the size, shape, and distribution of voids, inclusions and other defects during single and multiple laser, arc, or e-beam passes, and 3) Model validation focused on demonstrating a functional relationship between both the material composition and the AM processing parameters and resulting microstructure.

Material properties are dependent upon the microstructural characteristics of the part, while microstructure depends on the thermal gradients and cooling rates produced in the metal AM process. It is recognized that the material properties for AM parts are a strong function of the welding processing parameters. Thus, a fundamental understanding of how AM components behave in load-bearing applications depends critically on understanding the evolution of thermal (residual) stresses during component fabrication. The interaction of the residual stresses with localized stress concentrations and crack-like defects must also be taken into account to predict component reliability in load bearing and thermomechanical applications. In spite of solidification and melt pool dynamics influence the microstructure and defect development, the

ICCS Camera Ready Version 2019
To cite this paper please use the final published version:
DOI: 10.1007/978-3-030-22747-0_49

application of fundamental solidification theories to simulate the AM process has not been fully explored [8, 9]. Of the same manner, a strategy to the validation and assessment through the experimentation to demonstrate that the microstructure can be consistently and accurately predicted as a function of the processing parameters, is still required.

Several modelling techniques have been proposed in the literature [7-12]. Most of them are made to optimize the welding process input parameters by means of the finite element method (FEM). However, to control the formation of thermal cracks, distortion and porosity, a lot of hypothesis are introduced into the numerical analysis. In addition, due to the extreme cooling conditions, the events that follow welding are far from equilibrium and the formation of non-equilibrium phases cannot be avoided [13, 14]. On the other hand, the fine discretization required to capture field variable details in the vicinity of the moving heat source spot, increases the cost of the simulations. Moreover, the transient nature of the heat transfer problem considering the effect of multi-layer deposition on the prediction and validation of melting pool shape and thermal cycles, also increases the computational requirements. Currently, microstructure evolution models exist only for one melting and solidification step, such as would be encountered during an idealized (e.g., single pass) AM process. These simulations do not address the formation of non-equilibrium phases or the effect of multiple heating and cooling cycles, such as those encountered in production AM processes. In the present research, the mentioned effect and the heat loss (convection and radiation) between the weldment (layers) surfaces and the surroundings were included into the FE analysis.

Finite element thermo-plasticity multi-scale procedures in wire and arc AM process need to be developed. The thermo-mechanical analysis using non-standard domain decomposition methods based on the concept of Representative Volume Elements (RVEs) also needs to be addressed. The establishment of a methodology for characterizing direct energy deposited metals by linking processing variables to the resulting microstructure and subsequent material properties, is a pendent research goal. The present work aims to build a firm foundation for modeling thermal transport in wire + arc additive manufacturing process. The increasing use of state-of-the-art experimental techniques and also the increasing emphasis on the computation of unsteady flow phenomena are generating many highly informative moving flow sequences.

Industrially focused projects look for fundamental studies of modeling microstructure and stress formation across multiple scales. That is, thermal cycles at the macro, meso and micro-scale levels should be calculated to predict macro, meso and micro residual stresses. Although significant advances have been made, a multi-pass arc welding process has not yet been incorporated into a commercially available additive manufacturing system. It means that a fully automated system using wire + arc welding to additively manufacture metal components still need to be developed. In particular, the development of an automation software required to produce CAD-to-part capability is necessary. The focus of future work is also to integrate thermodynamics and materials thermo-mechanical modeling to provide a multidisciplinary solution to the control of microstructure, residual stress and surface finish in the DED-AM deposition process.

2 The thermal Model

The field variable temperature T(x; y; z; t) at any location (x; y; z) and time (t) with respect to the moving heat source is calculated by solving the heat diffusion equation:

$$\frac{\partial}{\partial x}\left(k\frac{\partial T}{\partial x}\right)+\frac{\partial}{\partial y}\left(k\frac{\partial T}{\partial y}\right)+\frac{\partial}{\partial z}\left(k\frac{\partial T}{\partial z}\right)+\dot{Q}=\rho c_p\frac{\partial T}{\partial t} \quad (1)$$

Here, ρ is the density, c_p is the specific heat, k is the thermal conductivity, T is temperature, t is time, and $\dot{Q}$ the internal heat source term. In the present research, $\dot{Q}$ is zero and the latent heat was not considered. The convective and radiative energy outflow is calculated with Eq. (2)

$$-k\frac{\partial T}{\partial y}|_{top}+q(r)=h_t(T-T_s)+\sigma\varepsilon(T^4-T_s^4) \quad (2)$$

Here, h_t =10 $Wm^{-2}K^{-1}$ is the convection coefficient at the workpiece surfaces, T_s is the surrounding temperature, ε is the emissivity and σ is the Stefan-Boltzman constant. Due to the flow of the shielding gas, the region directly beneath the nozzle of the torch experiences forced convection. In this area, a value of h_t= 242 W m^{-2} K^{-1} it was used. The ABAQUS [15] user subroutine FILM was constructed to account the convection and radiation effect, and the user subroutine DFLUX was written to account for the heat input from the moving heat source to the workpiece. The Gaussian power density distribution (Eq. 3) was used to represent the moving heat source. It was applied during a period of time that depends on the welding speed (v).

$$q(x,z,t)=\frac{3Q}{\pi C^2}exp^{\{-3[(z-vt)^2+x^2]/C^2\}} \quad (3)$$

Here, $Q=\eta Vi$, η is the process efficiency, V is voltage, i is electric current, and C is the heat distribution parameter.

ICCS Camera Ready Version 2019
To cite this paper please use the final published version:
DOI: 10.1007/978-3-030-22747-0_49

Table 1. Other data used in the simulations

Property	Value
Thermal efficiency (η)	0.7
T_o (room temperature)	20 °C
Density steel (ρ_w) at T_o	7820 Kg/m^3
Density alloy IN-738 at T_o	8110 Kg/m^3
Surface emissivity	0.7

3 The material model

It has been proved that thermal conductivity and specific heat change significantly when material is heated up to liquid phase from solid phase [16]. These physical properties for added material and solid substrate are also different. Therefore, the inclusion of these property changes in DED simulations is extremely important. As the velocity of the molten metal in the weld pool increases with temperature, an effective high thermal conductivity in the molten region was used to represent the weld pool stirring [1]. The physical properties of the SAE-AISI 1524 carbon steel used in reference [17] are plotted in Fig. 1.

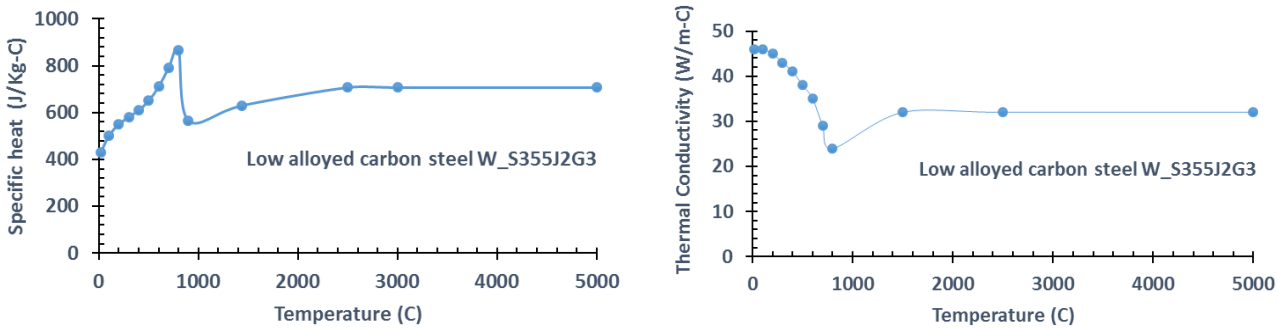

(a) (b)

Fig. 1. Physical properties of the SAE-AISI 1524 carbon steel (a) specific heat (b) thermal conductivity.

Of the same manner, the physical properties of cast IN-738LC alloy obtained from references [18, 19] are plotted in Fig. 2. Other properties used in the present research are summarized in Table 1. The influence of segregation and no equilibrium solidification was ignored in the FE analysis.

ICCS Camera Ready Version 2019
To cite this paper please use the final published version:
DOI: 10.1007/978-3-030-22747-0_49

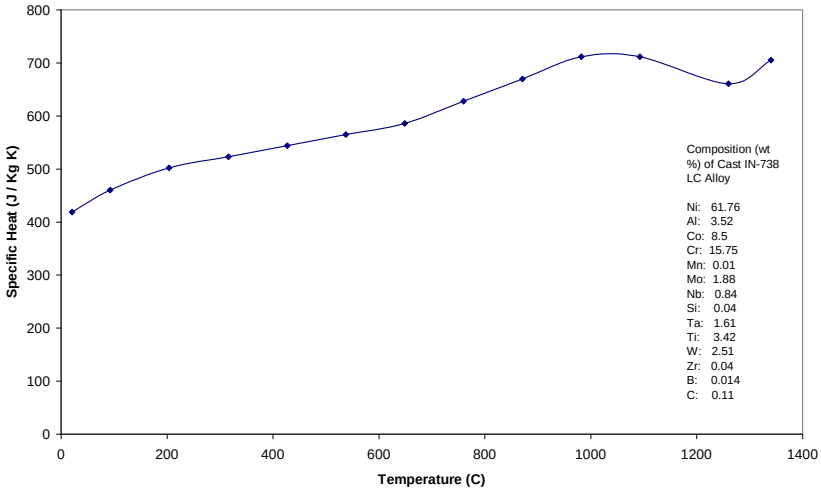

(a)

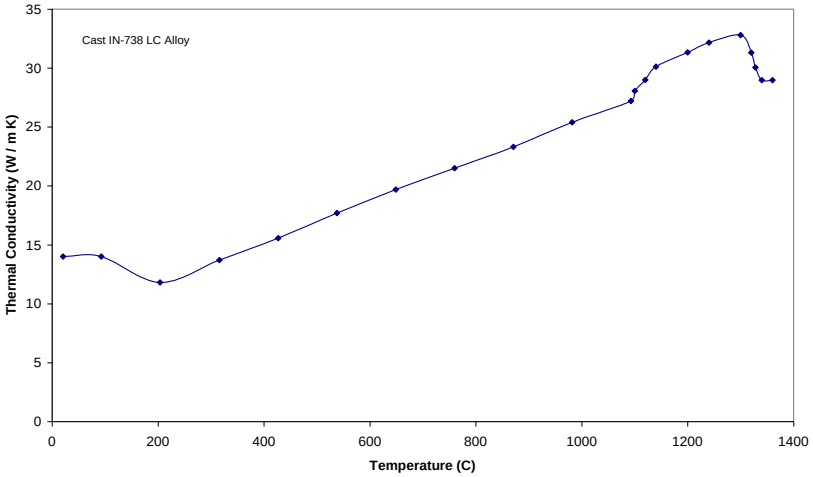

(b)

Fig. 2. Physical properties of cast IN-738LC alloy (a) specific heat (b) thermal conductivity.

To quantify the effect of the above process parameters and materials on the entire welding process, a 3D transient non-linear finite element model to simulate multi-layer deposition of cast IN-738LC alloy onto SAE-AISI 1524 carbon steel substrates was developed.

4 A physics-based method to describe the layer build-up process

To describe the layer build-up process, the continuous wire addition is based on the element-birth technique. A set of elements were added onto the substrate to form rectangular deposits as shown on Fig. 3. The width of the rectangular deposits depends on the heat distribution parameter *C*, and the thickness of the deposits depends on the wire feed rate and the heat source (arc) speed. For multiple arc passes, the corresponding boundary conditions were updated at the end of each time step. The order of deposition is: Layer a → Layer b → Layer c. That is, a new layer is deposited over a previously heated one.

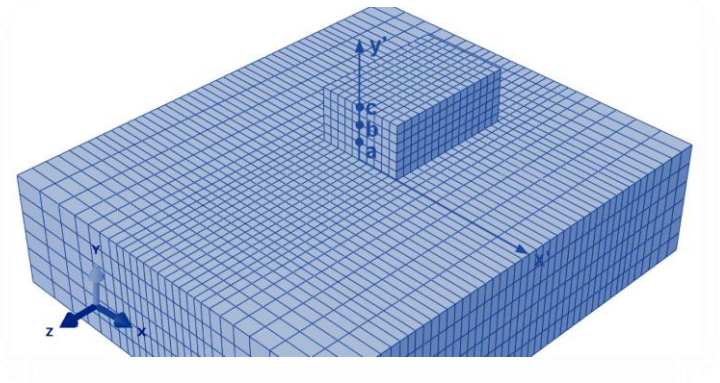

Fig. 3. Multiple arc passes meshing scheme created with the ABAQUS *MODEL CHANGE option.

ICCS Camera Ready Version 2019
To cite this paper please use the final published version:
DOI: 10.1007/978-3-030-22747-0_49

The layer build-up process was modeled by the following three steps: 1) the total mesh (substrate + filler metal layers) of the final DED part is created 2) all the elements within the filler metal layers are deactivated at the beginning of the simulation 3) the elements in the first filler metal layer are activated followed by the first arc scan. This process is repeated for the successive layers to approximate a real DED process, where filler metal is laid layer by layer after each scan. For future experimental work, it is expected that the filler metal depth be the same as the filler metal layer thickness used in the simulation. The sequence of the layer build-up process is shown in Fig. 4.

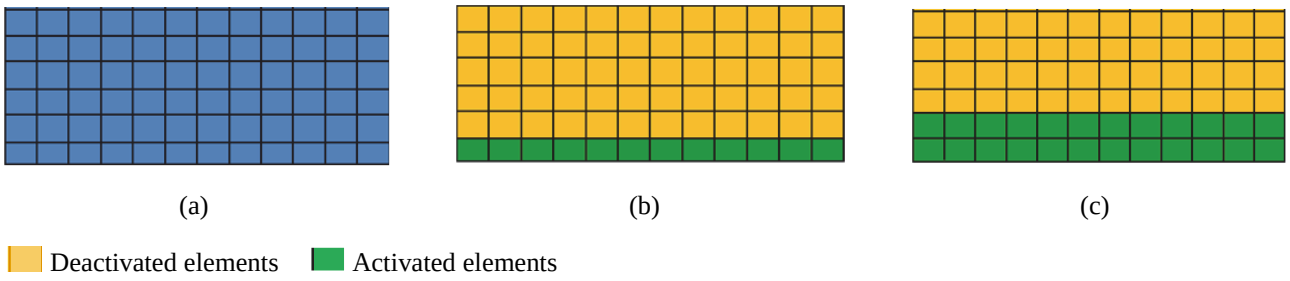

Fig. 4. a) Filler metal mesh b) Scan of 1st layer c) Scan of 2nd layer

5 The heat source material interaction

The calculations conducted in the present research are divided in two parts: In the *first part*, two AM tests (AM1 and AM2) were made using the welding parameters documented in Table 2. Two layers of filler metal (alloy IN-738) were deposited in a SAE-AISI 1524 carbon steel substrate. The heat distribution parameter, *C*, was determined based on the experimental measurement of the fusion zone width reported in Fig. 3 of reference [2]. The shape and distribution of the heat input greatly depends on its value. It is important to note that in this first part, convection and radiation heat loss from the layers surfaces *were not* included into the FE analysis.

Table 2. List of welding conditions used for processes AM1 and AM2

AM1	**Layer 1 (Weld1)**	**Layer 2 (Weld2)**
Voltage (Volts)	9.5	9.5
Intensity (Amps)	150	150
Heat Distribution parameter *C* (mm)	3.65	3.65
Weld velocity (mm/s)	2	2
AM2	**Layer 1 (Weld1)**	**Layer 2 (Weld2)**
Voltage (Volts)	10.5	10.5
Intensity (Amps)	200	200
Heat Distribution parameter *C* (mm)	5.3	5.3
Weld velocity (mm/s)	2	2

In the *second part*, two additional AM tests (AM3 and AM4) were made using the welding parameters documented in Table 3. Three layers of alloy IN-738 were deposited in a SAE-AISI 1524 carbon steel substrate. The effect of convection and radiation heat loss from the layers surfaces *were* included into the FE analysis.

Table 3. List of welding conditions used for processes AM3 and AM4

AM3	**Layer 1 (W1)**	**Layer 2 (W2)**	**Layer 3 (W3)**
Intensity (Amps)	150	100	50
Voltage (Volts)	10	10	10
Velocity (mm/s)	5.08	3.387	1.693
Heat distribution parameter *C* (mm)	4.5	4.5	3
AM4	**Layer 1 (W1)**	**Layer 2 (W2)**	**Layer 3 (W3)**
Intensity (Amps)	120	120	120
Voltage (Volts)	10	10	10
Velocity (mm/s)	3.125, 6.25 and 12. 5 in turn	3.125, 6.25 and 12. 5 in turn	3.125, 6.25 and 12. 5 in turn
Heat distribution parameter *C* (mm)	4.5	4.5	4.5

ICCS Camera Ready Version 2019
To cite this paper please use the final published version:
DOI: 10.1007/978-3-030-22747-0_49

To predict the evolution of temperature distribution in the entire weldment (substrate, two and three cast IN-738LC alloy layers) for the entire welding and cooling cycle of the process, a 3D transient nonlinear heat flow analysis was performed. To observe the heat transference among layers, all welding layers had gluing contacts. Fig. 5 shows the experimental set-up, specimen dimensions, and x, y and z directions for AM weld tests.

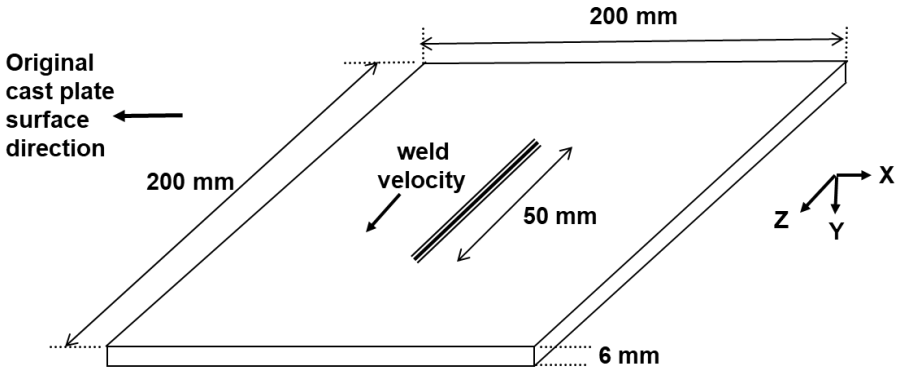

Fig. 5. Schematic of the experimental set-up for AM weld tests.

The initial temperature T_0 was set to 20 °C. The designed mesh is shown in Fig. 6a for processes AM1 and AM2, and in Fig. 6b for processes AM3 and AM4.

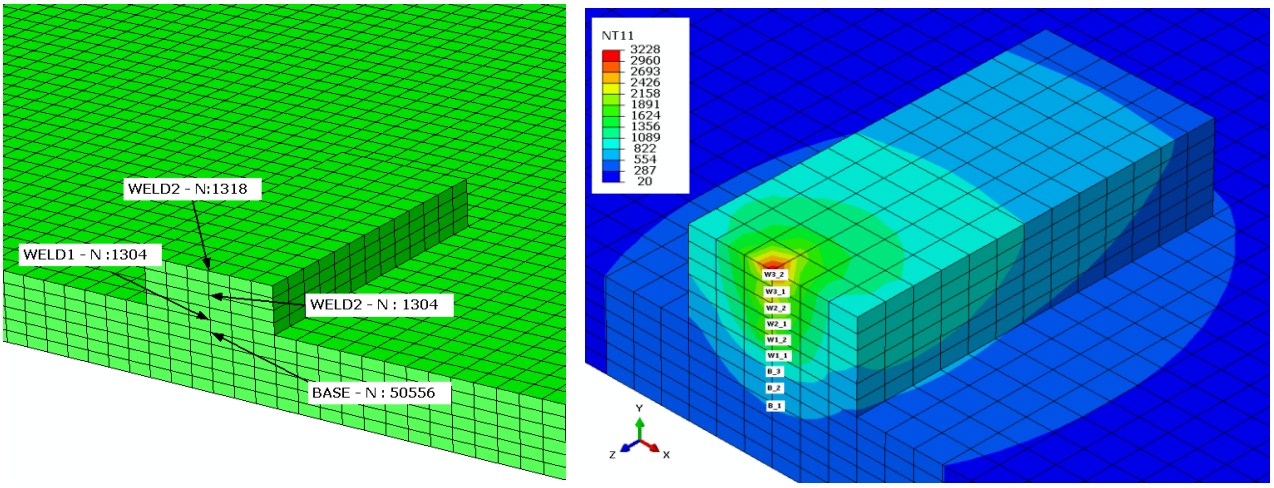

(a) (b)

Fig. 6. Selected nodes in a mesh composed of SAE-AISI 1524 Carbon Steel Substrate (200x6x200 mm) and layers of alloy IN-738 (12 x 2 x 50 mm each) a) Mesh used for processes AM1 and AM2 b) Mesh used for processes AM3 and AM4. The selected nodes are located in the central XY cross-sectional plane (i.e., from the top of cross section along Y axis). Element size 2x1x2 mm. Element type DC3D8.

6 Results and discussions

Numerically predicted thermal gradients, isotherms and thermal cycles produced by the AM process were calculated with the developed thermal model. For the *first part* of this work, the following results corresponding to the processes AM1 and AM2 were obtained in a mesh representing two wire layers (composed of four finite element rows) plus the substrate (Fig. 6a). The welding conditions used in the simulations are shown on Table 2. Fig. 7 shows thermal contourns and thermal cycles calculated at the reported nodes.

ICCS Camera Ready Version 2019
To cite this paper please use the final published version:
DOI: 10.1007/978-3-030-22747-0_49

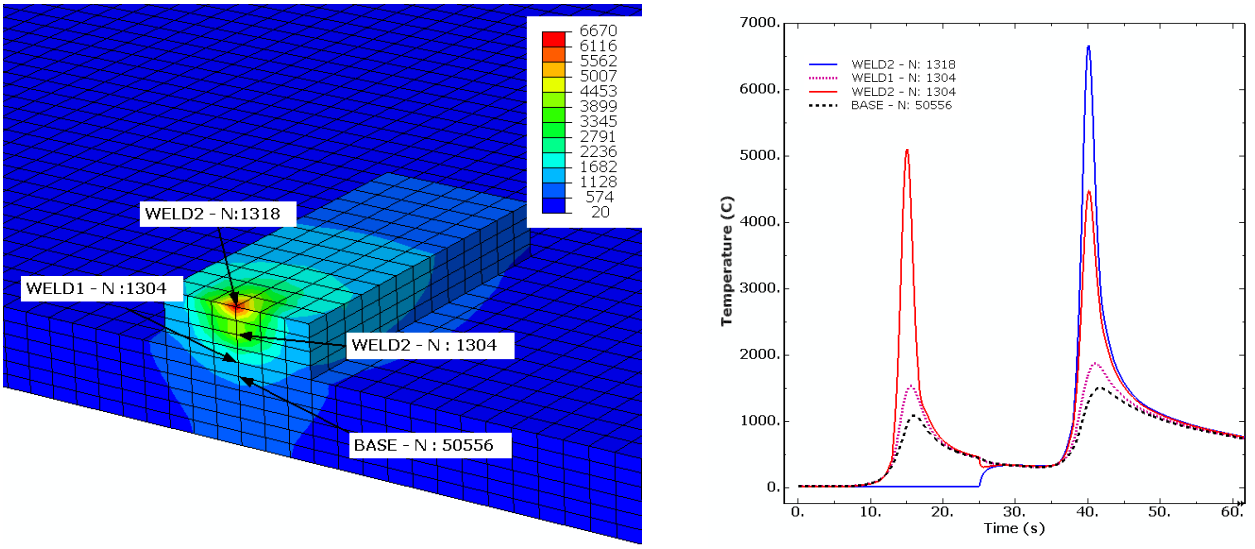

(a)

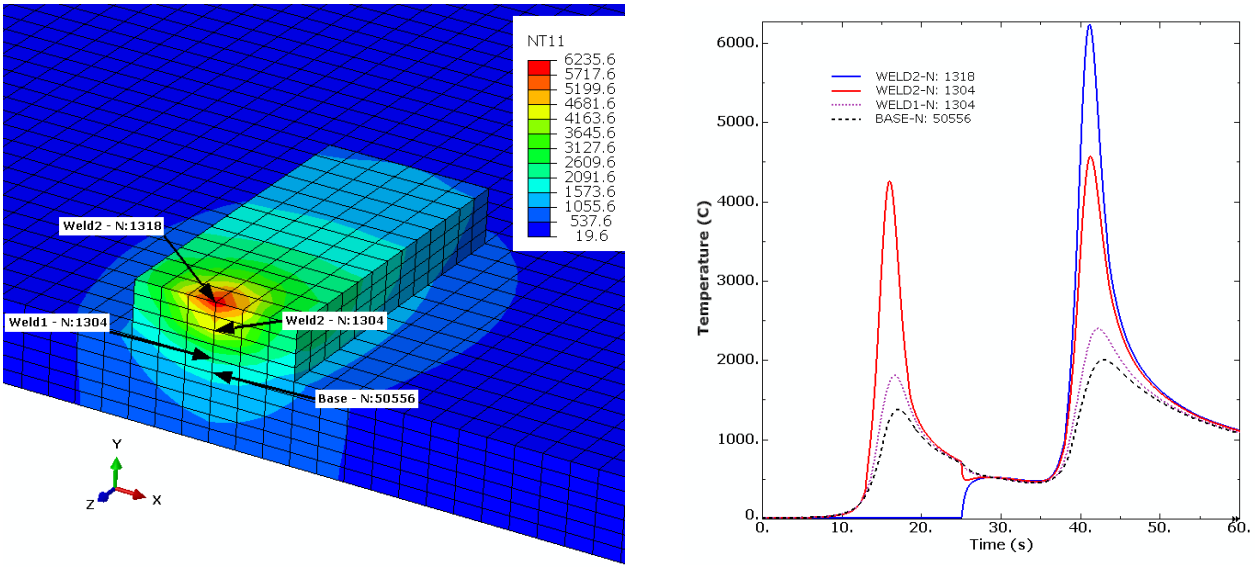

(b)

Fig. 7. Thermal contourns and thermal cycles for the AM process a) For the AM1 process b) For the AM2 process. Welding parameters documented in Table 2.

Compared with the AM2 process, higher peak temperatures are observed in the AM1 process. The reason is because in the AM1 process, a higher heat input is deposited to the workpiece.

The following results are obtained for the *second part* of this work. For instance, Fig. 8 shows thermal cycles calculated at the locations specified in Fig. 6b for process AM3. Even though the heat input is keep constant, it is apparent in Fig. 8 that as the weld velocity and heat distribution parameter decreases, the peak temperature increases. For these particular welding conditions, the effect of the heat distribution parameter is more representative.

ICCS Camera Ready Version 2019
To cite this paper please use the final published version:
DOI: 10.1007/978-3-030-22747-0_49

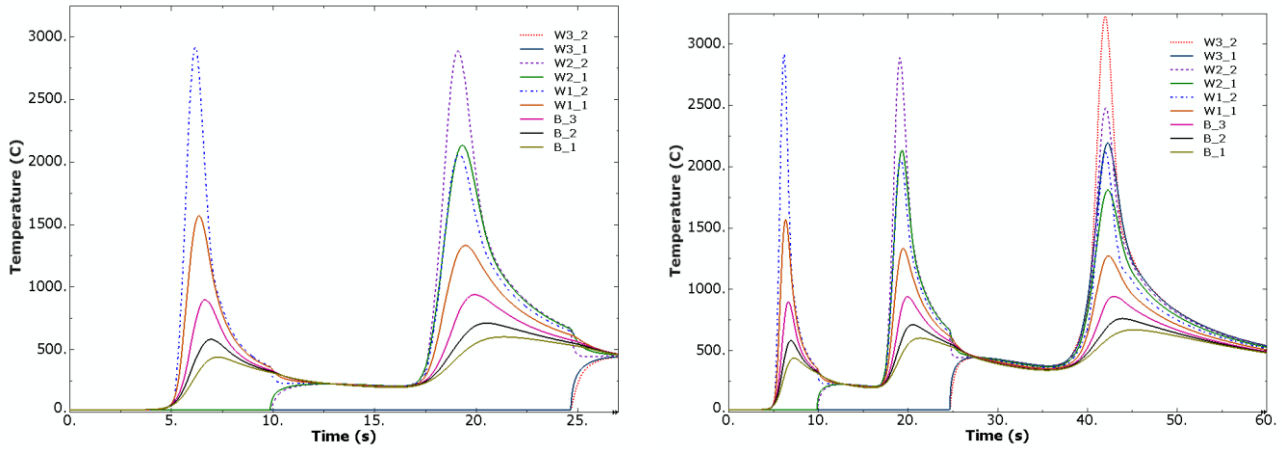

(a)

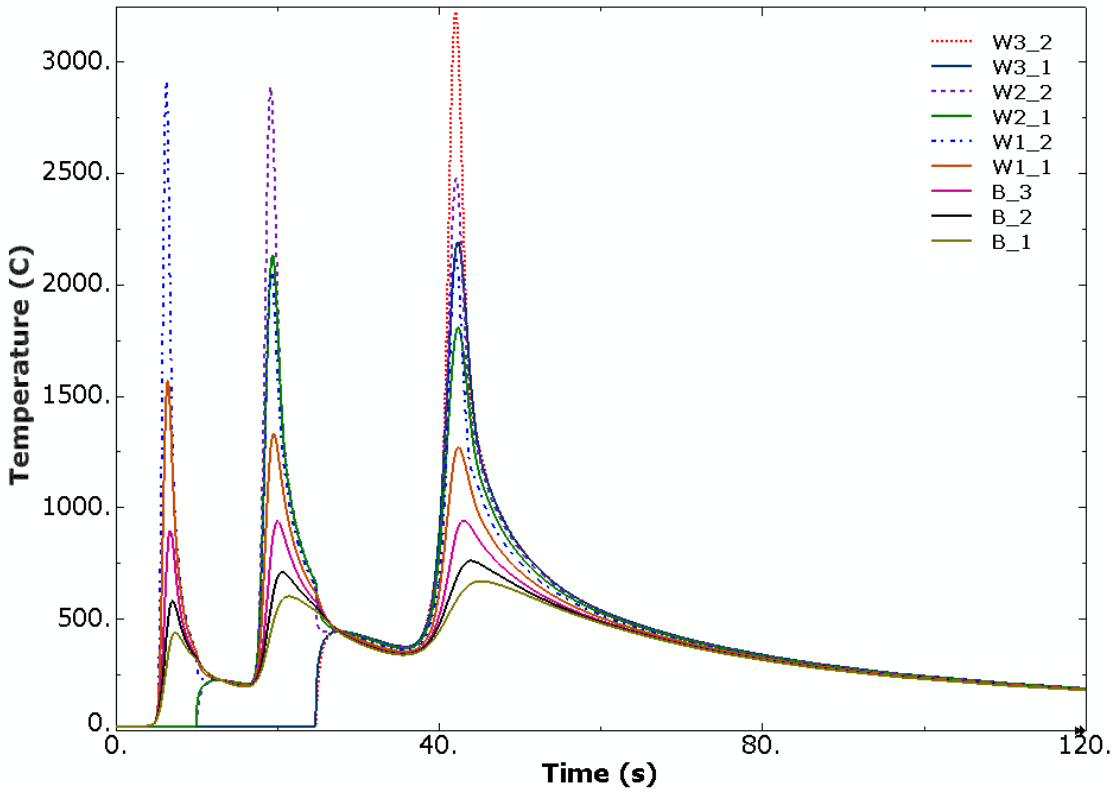

(b)

Fig. 8. Thermal cycles for the AM3 process a) Cooling time limited to 30 and 60 s b) Cooling time limited to 120 s. Welding parameters documented in Table 3.

Fig. 9 shows thermal cycles calculated at the reported nodes located in the substrate and in the three layers for the process AM4 at weld velocities of 12.5, 6.25 and 3.125 mm/s. The heat source is applied over the top surface of each layer (50 mm length) during a lapse of time that depends on the welding speed. The welding parameters are documented in Table 3.

ICCS Camera Ready Version 2019
To cite this paper please use the final published version:
DOI: 10.1007/978-3-030-22747-0_49

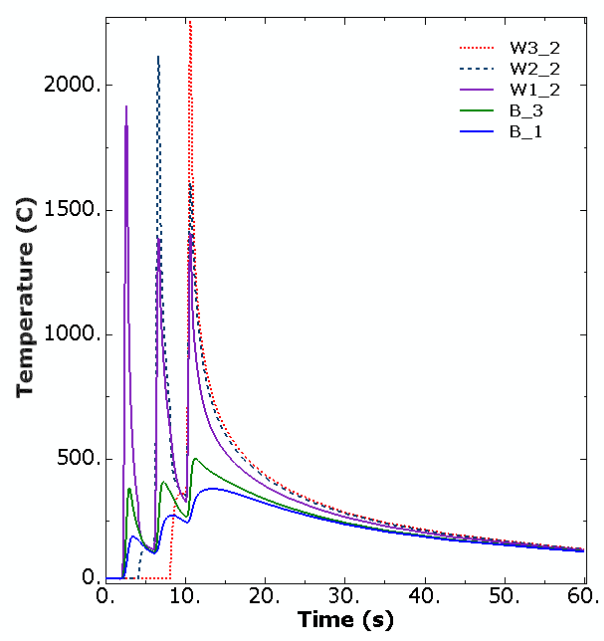

(a)

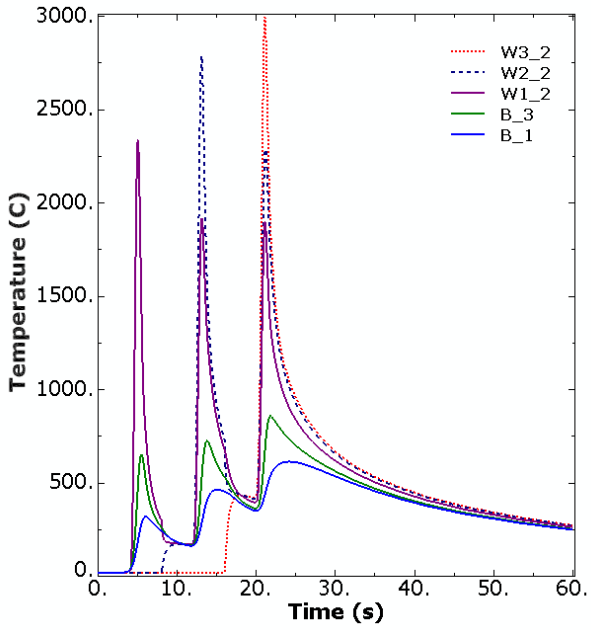

(b)

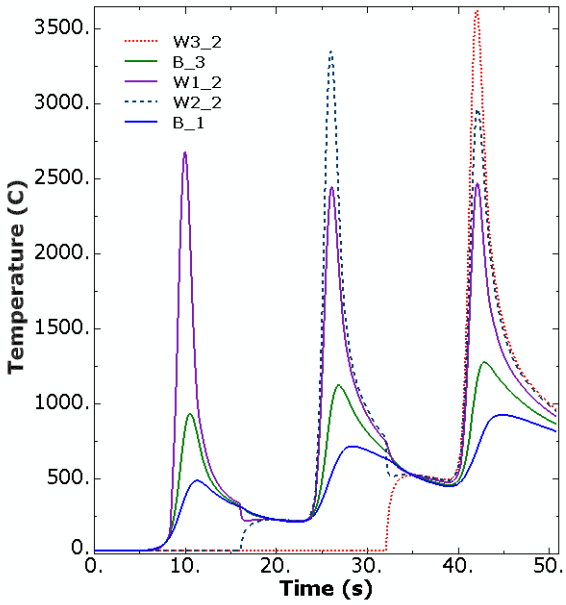

(c)

Fig. 9. Thermal cycles calculated at the reported nodes located in the substrate and in the three layers for different weld velocities a) For a weld velocity of 12.5 mm/s b) For a weld velocity of 6.25 mm/s c) For a weld velocity of 3.125 mm/s.

It is observed in Fig. 9 that as the weld velocity decreases, higher peak temperature arise. This is because the heat input (*HI*) described by Eq. (4), is inversely proportional to the weld velocity

$$HI = \frac{\eta V i}{v} \tag{4}$$

As stated above, η is the process efficiency, V is voltage, i is electric current, and v is the weld velocity. Of the same manner, as the heating and cooling curves are different in a same analyzed location, the corresponding mechanical properties will be different as different the AM process. It is necessary to mention that the thermal model is quite accurate to predict thermal cycles and weld zones profiles. It is also important to note that the peak temperatures calculated in the processes AM3 and AM4 considered in this *second part*, are smaller than those obtained in the *first part*, that is, in the processes AM1 and AM2. The reason is because the heat extraction by convection and radiation through the surfaces of

ICCS Camera Ready Version 2019
To cite this paper please use the final published version:
DOI: 10.1007/978-3-030-22747-0_49

the AM layers included into the FE analysis in the second part, is quite significant. The AM layers itself act as extended surfaces (fins).

7 Conclusions

1. A firm foundation for modeling thermal transport in wire + arc additive manufacturing process it was established.
2. A three dimensional transient non-linear finite element thermal model has been developed to generate weld profiles, thermal gradients, and thermal cycles in multi-layer deposition of cast IN-738LC alloy onto SAE-AISI 1524 Carbon Steel Substrates.
3. The effect of multi-layer deposition on the prediction and validation of melting pool shape and thermal cycles was also investigated.
4. The effect of convection and radiation heat loss from the layers surfaces were included into the FE analysis. As the AM layers itself act as extended surfaces (fins), it was found that the heat extraction is quite significant.
5. The developed thermal model is quite accurate to predict thermal cycles and weld zones profiles.

Acknowledgment

E. A. Bonifaz acknowledges to the Centro de Estudios e Investigaciones Técnicas de Guipuzcoa (CEIT) in Spain for allowing the use of its facilities during a short stay of scientific cooperation.

References

1. Bonifaz, E. A.: Finite element analysis of heat flow in single/pass arc welds. Welding Journal 79 (5), 121_s – 125_s (2000).
2. Bonifaz, E. A.: Thermo-mechanical analysis in SAE-AISI 1524 carbon steel gas tungsten arc welds. Int. J. Computational Materials Science and Surface Engineering 7 (3/4), 269-287 (2018).
3. Bonifaz E. A., Richards N. L.: Modeling Cast In-738 Superalloy Gas-Tungsten-Arc- Welds. Acta Materialia 57, 1785-1794 (2009).
4. Kou S.: Welding Metallurgy. 2nd ed. Wiley, New York (2003).
5. Bonifaz E. A., Richards N. L.: Stress-Strain Evolution in Cast IN-738 Superalloy Single Fusion Welds. International Journal of Applied Mechanics 2 (4), 807–826 (2010).
6. Brown, S. B., Song, H.: Implications of three-dimensional numerical simulations of welding of large structures. Welding Journal 71 (2), 55-s–62-s (1992).
7. Gibson, I., Rosen, D., Stucker, B.: Additive Manufacturing Technologies. Springer Science (2015).
8. Sames, W. J., List, F. A., Pannala, S., Dehoff, R., Babu, S. S.: The metallurgy and processing science of metal additive manufacturing. International Materials Reviews 61 (5), (2016).
9. Gu, D., Meiners, W., Wissenbach, K., Poprawe, R.: Laser additive manufacturing of metallic components: materials, processes and mechanisms. Journal International Materials Reviews 57 (3), 133-164 (2012).
10.http://www.farinia.com/additivemanufacturing/3dtechnique/modelingsimulationinmetaladditivemanufacturing
11. http://www.farinia.com/additivemanufacturing/3dtechnique/additivelayermanufacturing
12. Lindgren, L., Lundbäck, A., Fisk, M., Pederson, R., Andersson, J.: Simulation of additive manufacturing using coupled constitutive and microstructure models. Additive Manufacturing 12, 144–158 (2016).
13. Debroy, T., David, S. A.: Physical processes in fusion welding. Reviews of Modern Physics 67 (1), 85–112 (1995).
14. Thiessen, R. G., Richardson, I. M.: A physically based model for microstructure development in a macroscopic heat-affected zone: grain growth and recrystallization. Metall. Mater. Trans. B 37 (4), 655–663 (2006).
15. ABAQUS documentation manual, V. 6.12. Dassault Systèmes Simulia Corp., Providence, RI, USA.
16. Mudge, R. P., Wald, N. R.: Laser Engineered Net Shaping Advances Additive Manufacturing and Repair. Welding Journal 86 (1), 44-48 (2007).
17. SYSWELD-Visual Weld material data base. Material Database Manager (2011).
18. Alloy IN-738 Technical Data. INCO, the International Nickel Company, Inc. One New York Plaza, New York, N.Y. 10004.
19. J MatPro 4.1, Thermotech Sente Software © 2007, http://www.thermotech.co.uk/

ICCS Camera Ready Version 2019
To cite this paper please use the final published version:
DOI: 10.1007/978-3-030-22747-0_49